Single Cyano-Ligand-Bridged Mo(W)/S/Cu Cluster-Based Frameworks: Reactant- and Stoichiometry-Dependent Syntheses

Jinfang Zhang,[†] Yu Fang,[§] Yinlin Wang,[†] Weitao Chen,[†] Junyi Yang,[§] Yinglin Song,[§] Marie P. Cifuentes,[‡] Mark G. Humphrey,[‡] and Chi Zhang*[,†]

[†] *China-Australia Joint Research Center for Functional Molecular Materials, School of Chemical and Material Engineering, Jiangnan University, Wuxi 214122, P.R. China*

[§] *School of Physical Science and Technology, Soochow University, Suzhou 215006, P.R. China*

[‡] *Research School of Chemistry, Australian National University, Canberra, ACT 0200, Australia*

ABSTRACT: Five anionic single cyano-bridged Mo(W)/S/Cu cluster-based frameworks $\{[Pr_4N][WS_4Cu_3(CN)_2]\}_n$ (**1**), $\{[Pr_4N][WS_4Cu_4(CN)_3]\}_n$ (**2**), $\{[Pr_4N][WOS_3Cu_3(CN)_2]\}_n$ (**3**), $\{[Bu_4N][WOS_3Cu_3(CN)_2]\}_n$ (**4**) and $\{[Bu_4N][MoOS_3Cu_3(CN)_2]\}_n$ (**5**) were prepared by systematically varying the molar ratios of the starting materials, and the specific cations, cluster building blocks and central metal atoms in the cluster building blocks. **1** possesses an anionic 3D diamondoid framework constructed from 4-connected T-shaped clusters $[WS_4Cu_3]^+$ and single CN^- bridges. **2** is fabricated from 6-connected planar 'open' clusters $[WS_4Cu_4]^{2+}$ and single CN^- bridges, forming an anionic 3D architecture with an "ACS" topology. **3** and **4** exhibit novel anionic 2-D double-layer networks, both constructed from nest-shaped clusters $[WOS_3Cu_3]^+$ linked by single CN^- bridges, but containing the different cations $[Pr_4N]^+$ and $[Bu_4N]^+$, respectively. **5** is constructed from nest-shaped clusters $[MoOS_3Cu_3]^+$ and single CN^- bridges, with an anionic 3D diamondoid framework. Employing differing molar ratios of the reactants and varying the cluster building blocks resulted in differing single cyano-bridged Mo(W)/S/Cu cluster-based frameworks, while replacing the cation ($[Pr_4N]^+$ vs. $[Bu_4N]^+$) was found to have negligible impact on the nature of the framework. Unexpectedly, replacement of the central metal atom (W vs. Mo) in the cluster building blocks had a pronounced

effect on the framework. Nonlinear optical (NLO) properties of these single cyano-bridged Mo(W)/S/Cu cluster-based frameworks were investigated by the Z-scan techniques employing 4 ns pulses at 532 nm; **1**, **3** and **5** exhibit effective saturable absorption effects when irradiated by low-energy laser pulses, while **1**, **2** and **5** show strong nonlinear scattering properties when irradiated by high-energy laser pulses.

.....

Introduction

Cluster-based frameworks have attracted tremendous attention because of their intriguing architectures and topological networks,[1] as well as their applications as functional materials.[2] Most clusters studied thus far have fixed shape and connectivity (e.g. the tetranuclear 6-connected octahedral cluster $[Zn_4O(COO)_6]$[3] and the dinuclear 4-connected tetragonal cluster $[Cu_2(COO)_4]$[4]), which reduces the prospects for the formation of diverse and complex frameworks. Heterothiometallic clusters are an important kind of cluster that shows a rich array of cluster skeletons[5] with potential applications as nonlinear optical (NLO) materials and as models of the active sites of metalloenzymes and in catalyses.[6] Accordingly, heterothiometallic Mo(W)/S/Cu cluster-based frameworks have attracted increasing interest in recent years for their fascinating architectures[7] and applications in solvatochromism,[8] adsorption[9] and nonlinear optical (NLO) materials.[10] Many Mo(W)/S/Cu clusters, possessing a variety of skeletons and exhibiting diverse connectivity, have been constructed into frameworks; for example, the 4-connected T-shaped cluster $[WS_4Cu_3]^+$ has been employed to construct a 3D diamondoid network,[11] the 3D "ACS" and diamondoid frameworks can be constructed from 6- and 4-connected nest-shaped clusters $[MOS_3Cu_3]^+$ (M = Mo, W),[12] and the planar 'open' clusters $[WS_4Cu_4]^{2+}$ with 4- or 8-connectivity can be fabricated into 3D frameworks.[13]

While several effective methods (e.g. solid-state syntheses under mild thermolysis, solvothermal syntheses, preformed cluster syntheses, etc)[14] have been successfully developed to construct Mo(W)/S/Cu cluster-based frameworks, a systematic study of the effects of modifying the various reaction factors on the resultant Mo(W)/S/Cu cluster-based frameworks is lacking. Varying the reaction factors, such as the molar ratio of the starting materials, and the specific cation, cluster building block etc., may result in the achievement of Mo(W)/S/Cu clusters with different skeletons, and correspondingly distinct Mo(W)/S/Cu cluster-based architectures, which may inevitably lead to the modification or even subsequently decisive change in their physical properties.

In this study, we report the syntheses and single-crystal X-ray diffraction studies

of five anionic Mo(W)/S/Cu cluster-based frameworks supported by single CN^- bridges, namely $\{[Pr_4N][WS_4Cu_3(CN)_2]\}_n$ (**1**), $\{[Pr_4N][WS_4Cu_4(CN)_3]\}_n$ (**2**), $\{[Pr_4N][WOS_3Cu_3(CN)_2]\}_n$ (**3**), $\{[Bu_4N][WOS_3Cu_3(CN)_2]\}_n$ (**4**) and $\{[Bu_4N][MoOS_3Cu_3(CN)_2]\}_n$ (**5**). Several reaction factors (the molar ratio of the starting materials, and the specific cation, cluster building block and central metal atom) are shown to influence the resultant Mo(W)/S/Cu cluster-based frameworks. The NLO properties of these single cyano-bridged Mo(W)/S/Cu cluster-based frameworks have been determined by *Z*-scan experiments employing linearly polarized 4 ns laser pulses and varying energies at 532 nm.

Experimental section

The reactions and manipulations were conducted using standard Schlenk techniques under an atmosphere of argon. The starting materials $[NH_4]_2[WS_4]$ and $[NH_4]_2[MOS_3]$ (M = Mo, W) were obtained according to the literature procedures.[15] The solvents were carefully dried and distilled prior to use and other chemicals were commercially available and used as received. Elemental analyses for carbon, hydrogen and nitrogen were performed on a Perkin-Elmer 240C elemental analyzer. Infrared spectra were recorded with a Nicolet FT-170SX Fourier transform spectrometer (KBr pellets). Electronic spectra were measured on a Shimadzu UV-3100 spectrophotometer.

Preparation of $\{[Pr_4N][WS_4Cu_3(CN)_2]\}_n$ 1. Pr_4NI (0.63 g, 2.0 mmol), CuCN (0.27 g, 3.0 mmol), and NH_4SCN (0.46 g, 6.0 mmol) were added to 10 mL DMF and the resultant mixture was stirred for 5 min. $[NH_4]_2[WS_4]$ (0.35 g, 1 mmol) was then added to the above solution, and the reacting system was stirred for an additional 15 min. The resulting solution was then filtered and the orange filtrate was carefully layered with 1 mL DMF and 20 mL CH_3CN sequentially. Several days later, **1** was obtained as orange block crystals (yield: 0.26 g, 35% based on W). Anal. Calcd. for $C_{14}H_{28}Cu_3N_3S_4W$: C, 22.69; H, 3.81; N, 5.67%. Found: C, 22.77; H, 3.76; N, 5.61%. IR (KBr pellets, cm^{-1}): 2969(vs), 2142(vs), 2087(vs), 1472(vs), 1384(s), 462(vs), 439(vs).

Preparation of {[Pr_4N][$WS_4Cu_4(CN)_3$]}$_n$ 2. Pr_4NI (0.63 g, 2.0 mmol), CuCN (0.36 g, 4.0 mmol), and NH_4SCN (0.61 g, 8.0 mmol) were added to 12 mL DMF and the resultant mixture was stirred for 6 min. $[NH_4]_2[WS_4]$ (0.35 g, 1 mmol) was then added to the above solution, and the reacting system was stirred for an additional 15 min. The resulting solution was then filtered and the orange filtrate was carefully layered with 1 mL DMF and 20 mL CH_3CN sequentially. Several days later, **2** was obtained as orange block crystals (yield: 0.31 g, 37% based on W). Anal. Calcd. for $C_{15}H_{28}Cu_4N_4S_4W$: C, 21.69; H, 3.40; N, 6.74%. Found: C, 21.76; H, 3.35; N, 6.68%. IR (KBr pellets, cm^{-1}): 2970(vs), 2150(vs), 1471(vs), 1385(s), 442(vs).

Preparation of {[Pr_4N][$WOS_3Cu_3(CN)_2$]}$_n$ 3. Pr_4NI (0.63 g, 2.0 mmol), CuCN (0.27 g, 3.0 mmol), and NH_4SCN (0.46 g, 6.0 mmol) were added to 10 mL DMF and the resultant mixture was stirred for 5 min. $[NH_4]_2[WOS_3]$ (0.33 g, 1 mmol) was then added to the above solution, and the reacting system was stirred for an additional 15 min. The resulting solution was then filtered and the orange filtrate was carefully layered with 1 mL DMF and 20 mL CH_3CN sequentially. Several days later, **3** was obtained as yellow block crystals (yield: 0.23 g, 32% based on W). Anal. Calcd. for $C_{14}H_{28}Cu_3N_3OS_3W$: C, 23.19; H, 3.89; N, 5.80%. Found: C, 23.25; H, 3.85; N, 5.73%. IR (KBr pellets, cm^{-1}): 2971(vs), 2149(vs), 2095(vs), 1471(s), 1402(s), 922(vs), 439(vs).

Preparation of {[Bu_4N][$WOS_3Cu_3(CN)_2$]}$_n$ 4. Bu_4NBr (0.66 g, 2.0 mmol), CuCN (0.27 g, 3.0 mmol), and NH_4SCN (0.46 g, 6.0 mmol) were added to 10 mL DMF and the resultant mixture was stirred for 5 min. $[NH_4]_2[WOS_3]$ (0.33 g, 1 mmol) was then added to the above solution, and the reacting system was stirred for an additional 15 min. The resulting solution was then filtered and the orange filtrate was carefully layered with 1 mL DMF and 20 mL *i*-PrOH sequentially. Several days later, **4** was obtained as yellow block crystals (yield: 0.24 g, 31% based on W). Anal. Calcd. for $C_{18}H_{36}Cu_3N_3OS_3W$: C, 27.67; H, 4.64; N, 5.38%. Found: C, 27.72; H, 4.60; N, 5.34%. IR (KBr pellets, cm^{-1}): 2960(vs), 2142(vs), 1466(s), 1381(s), 923(vs), 441(vs).

Preparation of {[Bu_4N][$MoOS_3Cu_3(CN)_2$]}$_n$ 5. Bu_4NBr (0.66 g, 2.0 mmol), CuCN

(0.27 g, 3.0 mmol), and NH_4SCN (0.46 g, 6.0 mmol) were added to 10 mL DMF and the resultant mixture was stirred for 5 min. $[NH_4]_2[MoOS_3]$ (0.24 g, 1 mmol) was then added to the above solution, and the reacting system was stirred for an additional 15 min. The resulting solution was then filtered and the red filtrate was carefully layered with 1 mL DMF and 20 mL *i*-PrOH sequentially. Several days later, **5** was obtained as red block crystals (yield: 0.18 g, 26% based on Mo). Anal. Calcd. for $C_{18}H_{36}Cu_3MoN_3OS_3$: C, 31.18; H, 5.23; N, 6.06%. Found: C, 31.25; H, 5.19; N, 6.03%. IR (KBr pellets, cm^{-1}): 2961(vs), 2160(vs), 1470(s), 1400(s), 903(vs), 460(vs).

X-ray Structure Determination. Crystals of **1-5 s**uitable for single crystal X-ray analyses were obtained directly from the above preparations. All measurements were made on a Saturn 724+ CCD X-ray diffractometer by using Mo *Kα* (λ = 0.71070 Å). Single crystals of **1-5** were mounted with grease at the top of a glass fiber. Cell parameters were refined on all observed reflections by using the program *Crystalclear* (Rigaku Inc., 2007). The collected data were reduced by the program *Crystalclear* and an absorption correction (multiscan) was applied. The reflection data for **1-5** were also corrected for Lorentz and polarization effects. The crystal structures of **1-5** were solved by direct methods and refined on F^2 by full-matrix least-squares methods using the *SHELXTL* software package.[16] All non-hydrogen atoms except the disordered atoms were refined anisotropically. A summary of the key crystallographic information and their selected bond lengths and bond angles for **1-5** are listed in Tables 1 and S1-S5, respectively. CCDC 979147-979151.

Nonlinear Optical Measurements. The NLO properties of **1-5** were determined by performing *Z*-scan measurements.[17] Aniline solutions of **1** (2.15×10^{-4} mol dm^{-3}), **2** (4.14×10^{-4} mol dm^{-3}), **3** (4.92×10^{-4} mol dm^{-3}), **4** (5.12×10^{-4} mol dm^{-3}) and **5** (4.81×10^{-4} mol dm^{-3}) were placed in a 2 mm quartz cuvette for the NLO measurements, which were performed with linearly polarized 4 ns pulses with different energies at 532 nm generated from a Q-switched frequency-doubled Nd:YAG laser. **1-5** are stable toward air and laser light under the experimental conditions. The spatial profiles of the optical pulses were of nearly Gaussian transverse mode. The pulsed

laser was focused onto the sample cell with a 40 cm focal length mirror. The spot radius of the laser beam was measured to be 25 μm (half-width at $1/e^2$ maximum). The energy of the input and output pulses were measured simultaneously by precision laser detectors (Rjp-735 energy probes), which were linked to a computer by an IEEE interface,[18] while the incident pulse energy was varied by a Newport Com. Attenuator. The interval between the laser pulses was chosen to be 10 Hz to avoid the influence of thermal and long-term effects. The samples were mounted on a translation stage that was controlled by computer to move along the axis of the incident laser beam (*Z*-direction) with respect to the focal point. To determine both the sign and magnitude of the nonlinear refraction, a 2 mm diameter aperture was placed in front of the transmission detector and the transmittance recorded as a function of the sample position on the *Z*-axis (closed-aperture *Z*-scan). To measure the nonlinear absorption, the *Z*-dependent sample transmittance was taken without the aperture (open-aperture *Z*-scan).

Results and Discussion

Synthetic Procedure. A systematic examination of the effects of varying the starting material stoichiometry, and the types of cations, cluster building blocks and central metal atoms in cluster building blocks afforded architecturally diverse anionic single cyano-bridged Mo(W)/S/Cu cluster-based frameworks (Scheme 1). When the molar ratios of the starting materials and the cluster building blocks are varied, the resultant Mo(W)/S/Cu clusters usually exhibit different skeletons, and correspondingly distinct architectures. For example, two different 3-D single cyano-bridged W/S/Cu cluster-based frameworks **1** and **2**, fabricated from the 4-connected T-shaped clusters $[WS_4Cu_3]^+$ and 6-connected planar 'open' clusters $[WS_4Cu_4]^{2+}$, respectively, are obtained when the molar ratios of $[WS_4]^{2-}$ and CuCN are 1:3 and 1:4, respectively (Scheme 1). When the cluster building block $[WOS_3]^{2-}$ was used in the synthesis, a distinct 2-D double-layer architecture **3** that is based on nest-shaped $[WOS_3Cu_3]^+$ clusters was obtained (Scheme 1). Our previous work reveals that different solvent-coordinated cations direct the formation of W/S/Ag clusters possessing

isomeric skeletons.[19] While, the outcome is not cation-dependent, $[Pr_4N]^+$ and $[Bu_4N]^+$ forming the similar 2-D double-layer architectures **3** and **4**, respectively. The effect of replacing the cation $[Pr_4N]^+$ with $[Bu_4N]^+$ on the resultant single cyano-bridged Mo(W)/S/Cu cluster-based framework therefore appears negligible. W/S/Cu(Ag) cluster polymers and their Mo-containing counterparts usually have the same architectures. For instance $[Sr(DMAC)_6]_2[W_4S_{16}Ag_4]$ and $[Sr(DMAC)_6]_2[Mo_4S_{16}Ag_4]$ oligomers exhibit the same octanuclear planar"open" square-like arrangement;[6e] $\{[Et_4N]_2[WS_4Cu_4(CN)_4]\}_n$ and $\{[Et_4N]_2[MoS_4Cu_4(CN)_4]\}_n$ are fabricated by planar 'open' clusters $[MS_4Cu_4]^{2+}$ (M = Mo, W) and double CN^- bridges to form the same 3-D diamondoid networks.[13a] Unexpectedly, **5** exhibits a 3-D rather than a 2-D nest-shaped cluster-based framework (Scheme 1), although it was achieved through the same synthetic procedure as **4** except using $[NH_4]_2[MoOS_3]$ instead of $[NH_4]_2[WOS_3]$, consistent with replacement of the central metal atom (W vs. Mo) in the cluster building block strongly influencing the resultant single cyano-bridged Mo(W)/S/Cu cluster-based framework.

Crystal Structure of $\{[Pr_4N][WS_4Cu_3(CN)_2]\}_n$ (1). X-ray crystallographic analysis revealed that **1** crystallizes in the orthorhombic chiral space group $P2_12_12_1$, and exhibits an anionic non-interpenetrating 3-D architecture, constructed from T-shaped clusters $[WS_4Cu_3]^+$ and single CN^- bridges (Scheme 1, Figure 1). The asymmetric unit of **1** contains one $[WS_4Cu_3(CN)_2]^-$ moiety and one $[Pr_4N]^+$ cation. In each $[WS_4Cu_3]^+$ cluster, the W atom adopts a tetrahedral coordination geometry through bonding to two μ_2-S and two μ_3-S atoms (Figure 1a). The Cu atoms exhibit two kinds of coordination environment: Cu1 and Cu3 have triangular coordination geometries formed by one μ_2-S atom, one μ_3-S atom and one cyanide bridge, while Cu2 is coordinated by two μ_3-S atoms and two cyanide bridges, and possesses a tetrahedral geometry. The Cu1-W1-Cu3, Cu1-W1-Cu2 and Cu3-W1-Cu2 angles are 174.75(3), 89.24(3) and 85.63(3), respectively, giving rise to a nearly T-shaped arrangement for each $[WS_4Cu_3]^+$ cluster (Figure 1a). Each T-shaped building cluster in **1** is linked by another four $[WS_4Cu_3]^+$ units through single cyanide bridges (Figure 1a). From a

topological viewpoint, each T-shaped cluster can be regarded as a 4-connected node, the Schläfli symbol for which is 6^6; **1** therefore possesses a diamondoid topological network (Figure 1c). 1-D pseudo-square channels can be seen down the *c* axis (Figure 1b), while viewed along the *a* or *b* axes, the packing diagram of **1** reveals 1-D peanut-shaped channels (Scheme 1, Figure S1). The packing diagram in the [110] plane exhibits two kinds of irregular shaped channels, while both the building clusters and channels show an unusual ABCD stacking motif (Figure S2).

Crystal Structure of $\{[Pr_4N][WS_4Cu_4(CN)_3]\}_n$ (2). **2** crystallizes in the orthorhombic space group *P*nma, and possesses a novel anionic non-interpenetrating 3-D honeycomb framework (Scheme 1, Figure 2). The structure of **2** can be viewed as C_2 symmetric planar 'open' clusters $[WS_4Cu_4]^{2+}$ linked through single CN^- bridges in the [011] plane to create 2-D (4,4) nets, and then these 2-D nets stacking along the *a*-axis to afford a 3-D architecture sustained by CN^- pillars (Scheme S1). In each planar 'open' cluster $[WS_4Cu_4]^{2+}$, the W atom still adopts a tetrahedral coordination geometry, but this is formed through bonding to four μ_3-S atoms (Figure 2a). The four Cu atoms have triangular or tetrahedral coordination environments (Figure 2a). Each planar 'open' cluster $[WS_4Cu_4]^{2+}$ is linked to a further six $[WS_4Cu_4]^{2+}$ building clusters by single CN^- bridges (Figure 2a), the first occurrence of 6-connected $[WS_4Cu_4]^{2+}$ building clusters in Mo(W)/S/Cu(Ag) cluster-based coordination polymers.[8,13] Examination of the topology of **2** reveals an unusual 6-connected $4^9 6^6$ network, termed an "ACS" net (Figure 2d); this is the third example of an "ACS" net in the field of M/S/Cu(Ag) cluster-based coordination polymers.[10a,12a] The packing diagrams of **2** along the *b*- or *c*-axes show two kinds of irregular shaped channels with an ABAB stacking motif (Scheme 1, Figure 2c) while, viewed along the *a*-axis, the packing diagram of **2** reveals square-like channels (Figure 2b).

Crystal Structure of $\{[Pr_4N][WOS_3Cu_3(CN)_2]\}_n$ (3). **3** exhibits a novel anionic 2-D double-layer architecture (Scheme 1, Figure 3). In the nest-shaped cluster $[WOS_3Cu_3]^+$, the tetrahedrally-coordinated W atom is linked to one terminal O and three μ_3-S atoms (Figure 3a), while the three Cu atoms have two distinct coordination

environments: Cu1 has a tetrahedral coordination environment, being bonded to two μ_3-S atoms and two cyanide bridges, and Cu2 and Cu3 have triangular coordination geometries, formed by two μ_3-S atoms and one cyanide bridge (Figure 3a). Each nest-shaped cluster $[WOS_3Cu_3]^+$ is connected to another four nest-shaped building clusters by single CN^- bridges, resulting in a 2-D (4,4) network (Figure 3a). Interestingly, this 2-D (4,4) network exhibits a double-layer arrangement (Figures 3b, 3c), the first time that such an arrangement has been seen in Mo(W)/S/Cu(Ag) cluster-based coordination polymers.[5a,7-14]

Crystal Structure of $\{[Bu_4N][WOS_3Cu_3(CN)_2]\}_n$ (4). Structural analysis revealed that **4** crystallizes in the monoclinic space group $P2_1/c$, and the asymmetric unit contains two crystallographically independent $[WOS_3Cu_3(CN)_2]^-$ moieties and two $[Bu_4N]^+$ cations. Each crystallographically-independent nest-shaped cluster $[WOS_3Cu_3]^+$ links another four $[WOS_3Cu_3]^+$ units through single CN^- bridges to form a 2-D double-layer (4,4) network similar to that in **3** (Figure 4).

Crystal Structure of $\{[Bu_4N][MoOS_3Cu_3(CN)_2]\}_n$ (5). X-ray crystallographic analysis revealed that **5** crystallizes in the orthorhombic chiral space group $P2_12_12_1$ with a 3-D anionic non-interpenetrating framework; this is fabricated by linking nest-shaped clusters $[MoOS_3Cu_3]^+$ through single CN^- bridges to afford 2D (6,3) nets in the [101] plane, and then these 2D (6,3) nets stack along the *b*-axis to give a 3-D architecture supported by CN^- pillars (Scheme S2). The asymmetric unit of **5** contains one $[MoOS_3Cu_3(CN)_2]^-$ moiety and one $[Bu_4N]^+$ cation. Each nest-shaped cluster $[MoOS_3Cu_3]^+$ in **5** exhibits the same 4-connected motif as the nest-shaped clusters $[WOS_3Cu_3]^+$ in **3** and **4** (Figure 5a), but with a distinct 3-D architecture rather than the 2-D double-layer networks seen in **3** and **4** (Scheme 1, Figures 5b, 5c). Topological analysis reveals that **5** possesses a diamondoid network with the Schläfli symbol 6^6 (Figure 5d). Packing diagrams of **5** viewed along the a-, *b*- or *c*-axes reveal irregular shaped channels (Scheme 1, Figures 5b, 5c).

Nonlinear Optical Properties. The UV-vis absorption spectra of **1-5** show relatively low linear absorption in the visible and near-IR region (Figures S4-S8), suggesting

that these clusters may potentially exhibit NLO properties. To assess this possibility, Z-scan experiments employing linearly polarized 4 ns duration 532 nm laser pulses with varying energies were performed on **1-5** in aniline solutions.[17] When irradiated by low-energy laser pulses (1.5 μJ for **1** and **5**, 1.6 μJ for **3**), **1**, **3** and **5** exhibit saturable absorption effects (Figures S9-S11). Reasonable fits between the experimental data and theoretical curves were achieved, from which the nonlinear absorptive coefficients a_2 were calculated to be -3.64×10^{-11} m W^{-1} for **1**, -3.20×10^{-11} m W^{-1} for **3** and -4.35×10^{-11} m W^{-1} for **5**, suggesting that they are possible candidates for NLO materials. When irradiated by high-energy laser pulses (15 μJ for **1** and **5**, 16 μJ for **2**), **1**, **2** and **5** show strong nonlinear scattering properties (Figures S12-S14). Again, reasonable fits between the experimental data and the theoretical curves were achieved, from which the nonlinear absorptive coefficients a_2 were calculated to be 8.2×10^{-11} m W^{-1} for **1**, 3.3×10^{-10} m W^{-1} for **2** and 8.1×10^{-10} m W^{-1} for **5**, and consistent with the solution species exhibiting potential in optical limiting.

Conclusions

The findings reported herein demonstrate that the syntheses of anionic single cyano-bridged Mo(W)/S/Cu cluster-based frameworks are affected by diverse reaction factors. Different molar ratios of the starting materials and varying the nature of the cluster building blocks result in distinct Mo(W)/S/Cu cluster skeletons, and thereby influences the resultant Mo(W)/S/Cu cluster-based frameworks, while the effect of varying the cation ($[Pr_4N]^+$ vs $[Bu_4N]^+$) on the single cyano-bridged Mo(W)/S/Cu cluster-based frameworks was found to be negligible. Replacement of the central metal atoms (W cf. Mo) in the cluster building blocks was shown to have a pronounced effect on the single cyano-bridged Mo(W)/S/Cu cluster-based framework. Finally, preliminary studies of NLO behavior revealed that **1**, **3** and **5** exhibit saturable absorption effects when irradiated by low-energy laser pulses, whereas **1**, **2** and **5** show strong nonlinear scattering properties when irradiated by high-energy laser pulses.

Acknowledgment

This research was financially supported by the National Natural Science Foundation of China (50925207, 51172100), the Ministry of Science and Technology of China (2011DFG52970), the Ministry of Education of China for the Changjiang Innovation Research Team (IRT1064), the Ministry of Education and the State Administration of Foreign Experts Affairs for the 111 Project (B13025), Jiangsu Innovation Research Team, and the Fundamental Research Funds for the Central Universities (JUSRP1022). M.G.H. thanks the Australian Research Council for support.

Supporting Information

Schemes S1-S2, illustrating the formation of the 3D anionic frameworks of **2** and **5**; Figures S1-S3, showing the 3D anionic frameworks of **1** and **2**; Figures S4-S8, displaying the UV-vis spectra of **1**-**5**; Figures S9-S11, showing open-aperture Z-scan measurements of **1**, **2** and **5** at 532 nm with low-energy laser pulses; Figures S12-S14, displaying open-aperture Z-scan measurements of **1, 3** and **5** at 532 nm with high-energy laser pulses; Tables S1-S5, listing selected bond distances and bond angles for **1**-**5**; and X-ray crystallographic information files (CIFs) for **1**-**5** are available. This information is available free of charge via the Internet at http://pubs.acs.org.

References:

1. (a) Schoedel, A.; Boyette, W.; Wojtas, L.; Eddaoudi, M.; Zaworotko, M. J. *J. Am. Chem. Soc.* **2013**, *135*, 14016-14019. (b) Wang, X. L.; Qin, C.; Wu, S. X.; Shao, K. Z.; Lan, Y. Q.; Wang, S.; Zhu, D. X.; Su, Z. M.; Wang, E. B. *Angew. Chem., Int. Ed.* **2009**, *48*, 5291-5295. (c) Zhang, X. M.; Lv, J.; Ji, F.; Wu, H. S.; Jiao, H. J.; Schleyer, P. v. R. *J. Am. Chem. Soc.* **2011**, *133*, 4788-4790. (d) He, H.; Cao, G. J.; Zheng, S. T.; Yang, G. Y. *J. Am. Chem. Soc.* **2009**, *131*, 15588-15589.
2. (a) Murray, L. J.; Dincă, M.; Long, J. R. *Chem. Soc. Rev.* **2009**, *38*, 1294-1314. (b) Zheng, B. S.; Bai, J. F.; Duan, J. G.; Wojtas, L.; Zaworotko, M. J. *J. Am. Chem. Soc.* **2011**, *133*, 748-751. (c) Kang, Y.; Wang, F.; Zhang, J.; Bu, X. H. *J. Am. Chem. Soc.* **2012**, *134*, 17881-17884. (d) Furukawa, H.; Ko, N.; Go, Y. B.; Aratani, N.; Choi, S. B.; Choi, E.; Yazaydin, A. O.; Snurr, R. Q.; O'Keeffe, M.; Kim, J.; Yaghi, O. M. *Science* **2010**, *329*, 424-428. (e) Yan, Y.; Telepeni, I.; Yang, S. H.; Lin, X.; Kockelmann, W.; Dailly, A.; Blake, A. J.; Lewis, W.; Walker, G. S.; Allan, D. R.; Barnett, S. A.; Champness, N. R.; Schröder, M. *J. Am. Chem. Soc.* **2010**, *132*, 4092-4094. (f) Sen, S.; Nair, N. N.; Yamada, T.; Kitagawa, H.; Bharadwaj, P. K. *J. Am. Chem. Soc.* **2012**, *134*, 19432-19437.
3. (a) Rowsell, J. L. C.; Spencer, E. C.; Eckert, J.; Howard, J. A. K.; Yaghi, O. M. *Science* **2005**, *309*, 1350-1354. (b) Yue, Q.; Sun, Q.; Cheng, A. L.; Gao, E. Q. *Cryst. Growth Des.* **2010**, *10*, 44-47. (c) Kesanli, B.; Cui, Y.; Smith, M. R.; Bittner, E. W.; Bockrath, B. C.; Lin, W. B. *Angew. Chem., Int. Ed.* **2005**, *44*, 72-75.
4. (a) Cai, J. F.; Rao, X. T.; He, Y. B.; Yu, J. C.; Wu, C. D.; Zhou, W.; Yildirim, T.; Chen, B. L.; Qian, G. D. *Chem. Commun.* **2014**, *50*, 1552-1554. (b) Ma, H. Q.; Sun, D.; Zhang, L. L.; Wang, R. M.; Blatov, V. A.; Guo, J.; Sun, D. F. *Inorg. Chem.* **2013**, *52*, 10732-10734. (c) Gao, W. Y.; Wojtas, L.; Ma, S. Q. *Chem. Commun.* **2014**, *50*, 10.1039/c3cc47542e.
5. (a) Niu, Y. Y.; Zheng, H. G.; Hou, H. W.; Xin, X. Q. *Coord. Chem. Rev.* **2004**, *248*, 169-183. (b) Zhang, C.; Jin, G. C.; Chen, J. X.; Xin, X. Q.; Qian, K. P. *Coord. Chem. Rev.* **2001**, *213*, 51-77. (c) Hou, H. W.; Xin, X. Q.; Shi, S. *Coord. Chem. Rev.* **1996**, *153*, 25-56.

6. (a) Zhang, C.; Song, Y. L.; Wang, X. *Coord*. *Chem*. *Rev*. **2007**, *251*, 111-141. (b) Shi, S.; Ji, W.; Tang, S. H.; Lang, J. P.; Xin, X. Q. *J*. *Am*. *Chem*. *Soc*. **1994**, *116*, 3615-3616. (c) Zhang, C.; Song, Y. L.; Kühn, F. E.; Wang, Y. X.; Xin, X. Q.; Herrmann, W. A. *Adv*. *Mater*. **2002**, *14*, 818-822. (d) Zhang, C.; Song, Y. L.; Fung, B. M.; Xue, Z. L.; Xin, X. Q. *Chem*. *Commun*. **2001**, 843-844. (e) Zhang, J. F.; Meng, S. C.; Song, Y. L.; Zhao, H. J., Li, J. H.; Qu, G. J.; Sun, L.; Humphrey, M. G.; Zhang, C. *Chem. Eur. J.* **2010**, *16*, 13946-13950. (f) Müller, A.; Diemann, E.; Jostes, R.; Bogge, H. *Angew*. *Chem*. *Int*. *Ed*. *Engl*. **1981**, *20*, 934-955. (g) Coucouvanis, D. *Acc*. *Chem*. *Res*. **1991**, *24*, 1-8. (h) Lee, S. C.; Holm, R. H. *Chem*. *Rev*. **2004**, *104*, 1135-1158. (i) Stiefel, E. I.; Matsumoto, K. *Transition Metal Sulfur Chemistry*: *Biological and Industrial Significance*, American Chemical Society, Washington, DC, **1996**. (j) Dance, I.; Fisher, K. *Prog*. *Inorg*. *Chem*. **1994**, *41*, 637-803. (k) Holm, R. H. *Adv*. *Inorg*. *Chem*. **1992**, *38*, 1-71.

7. (a) Liang, K.; Zheng, H. G.; Song, Y. L.; Lappert, M. F.; Li, Y. Z.; Xin, X. Q.; Huang, Z. X.; Chen, J. T.; Lu, S. F. *Angew*. *Chem*. *Int*. *Ed*. **2004**, *43*, 5776-5779. (b) Lu, Z. Z.; Zhang, R.; Li, Y. Z.; Guo, Z. J.; Zheng, H. G. *Chem*. *Commun*. **2011**, *47*, 2919-2921.

8. Lu, Z. Z.; Zhang, R.; Li, Y. Z.; Guo, Z. J.; Zheng, H. G. *J. Am. Chem. Soc*. **2011**, *133*, 4172-4174.

9. Lang, J. P.; Xu, Q. F.; Yuan, R. X.; Abrahams, B. F. *Angew. Chem., Int. Ed.* **2004**, *43*, 4741-4745.

10. (a) Zhang, C.; Cao, Y.; Zhang, J. F.; Meng, S. C.; Matsumoto, T.; Song, Y. L.; Ma, J.; Chen, Z. X.; Tatsumi, K.; Humphrey, M. G. *Adv*. *Mater*. **2008**, *20*, 1870-1875. (b) Chen, X.; Li, H. X.; Zhang, Z. Y.; Zhao, W.; Lang, J. P.; Abrahams, B. F. *Chem. Commun*. **2012**, *48*, 4480-4482. (c) Yao, X. Q.; Pan, Z. R.; Hu, J. S.; Li, Y. Z.; Guo, Z. J.; Zheng, H. G. *Chem*. *Commun*. **2011**, *47*, 10049-10051.

11. Zhang, J. F.; Song, Y. L; Yang, J. Y.; Humphrey, M. G.; Zhang, C. *Cryst. Growth Des*. **2008**, *8*, 387-390.

12. (a) Zhang, J. F.; Meng, S. C.; Song, Y. L; Zhou, Y. M.; Cao, Y.; Li, J. H.; Zhao, H. J.; Hu, J. C.; Wu, J. H.; Humphrey, M. G.; Zhang, C. *Cryst*. *Growth Des*. **2011**, *11*,

100-109. (b) Huang, K. X.; Song, Y. L.; Pan, Z. R.; Li, Y. Z.; Zhuo, X.; Zheng, H. G. *Inorg*. *Chem*. **2007**, *46*, 6233-6235. (c) Liang, K.; Zheng, H. G.; Song, Y. L.; Li, Y. Z.; Xin, X. Q. *Cryst*. *Growth Des*. **2007**, *7*, 373-376.

13. (a) Lu, Z. Z.; Zhang, R.; Pan, Z. R.; Li, Y. Z.; Guo, Z. J.; Zheng, H. G. *Chem. Eur. J.* **2012**, *18*, 2818-2824. (b) Zhang, C.; Song, Y. L.; Xu, Y.; Fun, H. K.; Fang, G. Y.; Wang, Y. X.; Xin, X. Q. *J*. *Chem*. *Soc*., *Dalton Trans*. **2000**, 2823-2829. (c) Zhang, W. H.; Lang, J. P.; Zhang, Y.; Abrahams, B. F. *Cryst*. *Growth Des*. **2008**, *8*, 399-401.
14. (a) Cai, Y.; Wang, Y.; Li, Y. Z.; Wang, X. S.; Xin, X. Q.; Liu, C. M.; Zheng, H. G. *Inorg*. *Chem*. **2005**, *44*, 9128-9130. (b) Song, L.; Li, J. R.; Lin, P.; Li, Z. H.; Li, T.; Du, S. W.; Wu, X. T. *Inorg*. *Chem*. **2006**, *45*, 10155-10161. (c) Pan, Z. R.; Xu, J.; Zheng, H. G.; Huang, K. X.; Li, Y. Z.; Guo, Z. J.; Batten, S. R. *Inorg*. *Chem*. **2009**, *48*, 5772-5778. (d) Lang, J. P.; Jiao, C. M.; Qiao, S. B.; Zhang, W. H.; Abrahams, B. F. *Inorg*. *Chem*. **2005**, *44*, 3664-3668. (e) Han, Y.; Zhang, Z. H.; Liu, Y. Y.; Niu, Y. Y.; Ding, D. G.; Wu, B. L.; Hou, H. W.; Fan, Y. T. *Cryst*. *Growth Des*. **2011**, *11*, 3448-3455. (f) Wang, H. M.; Han, Y.; Niu, Y. Y.; Zhang, Z. H.; Hou, H. W.; Zhu, Y. *CrystEngComm* **2012**, *14*, 3125-3130. (g) Chen, J. X.; Tang, X. Y.; Chen, Y.; Zhang, W. H.; Li, L. L.; Yuan, R. X.; Zhang, Y.; Lang, J. P. *Cryst*. *Growth Des*. **2009**, *9*, 1461-1469.
15. McDonald, J. W.; Frieson, G. D.; Rosenhein, L. D.; Newton, W. E. *Inorg*. *Chim*. *Acta* **1983**, *72*, 205-210.
16. Sheldrick, G. M. *SHELXS-97* and *SHELXL-97*, *Programs for Crystal Structure Refinement*, University of Göttingen, Germany, 1997.
17. Sheik-Bahae, M.; Said, A. A.; Wei, T. H.; Hagan, D. J.; Van Stryland, E. W. *IEEE J*. *Quantum Electron*. **1990**, *26*, 760-769.
18. Sheik-Bahae, M.; Hutchings, D. C.; Hagan, D. J.; Van Stryland, E. W. *IEEE J*. *Quantum Electron*. **1991**, *27*, 1296-1309.

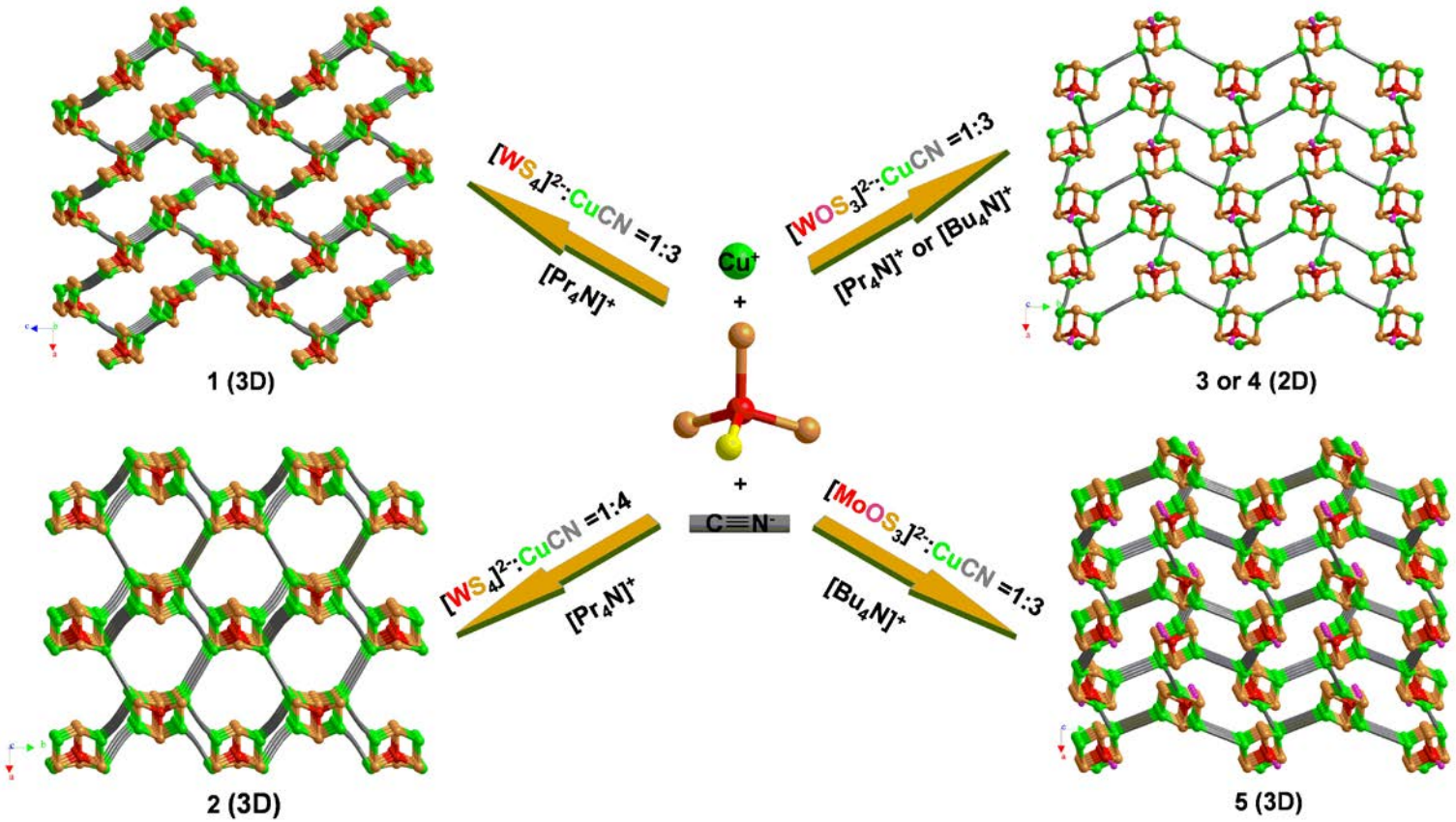

Scheme 1. Syntheses of **1-5** (gray sticks represent the CN^- bridges, and orange, red, pink, and green balls represent S, W or Mo, O, and Cu atoms, respectively).

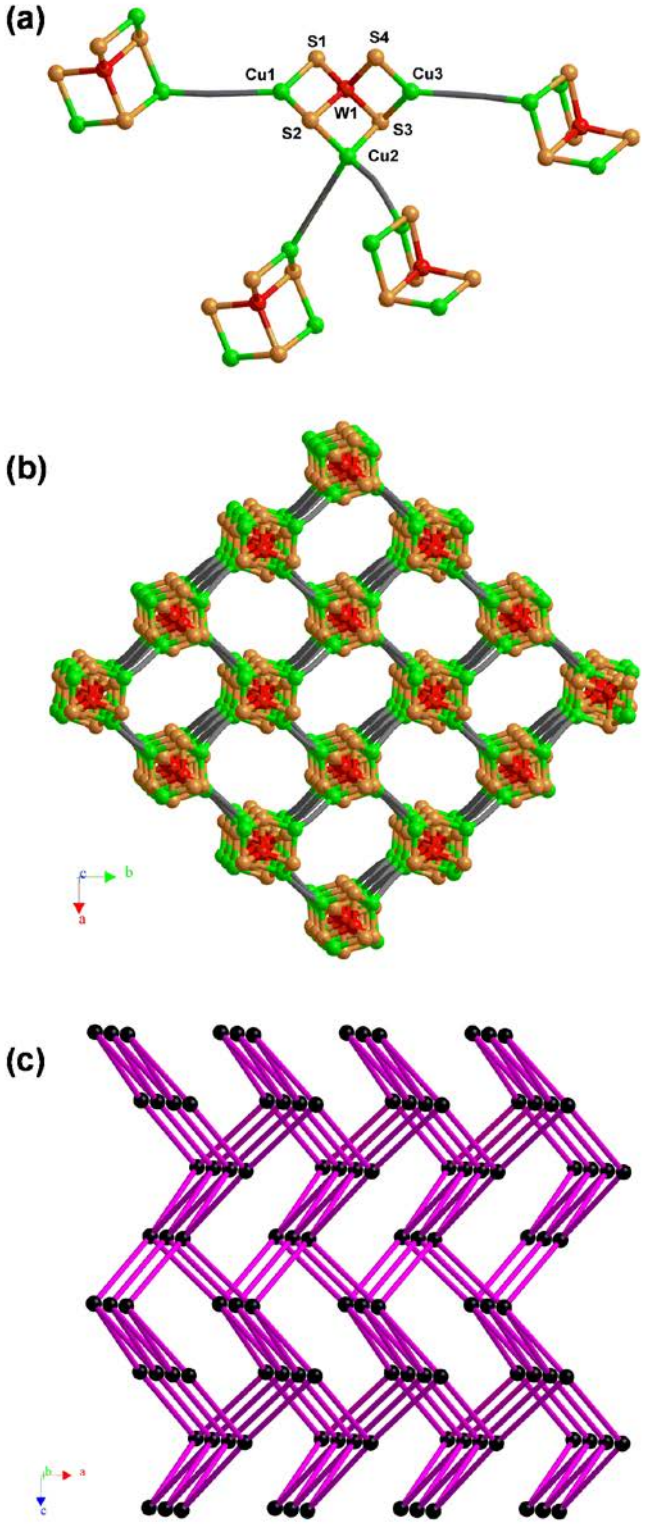

Figure 1. (a) Partial view of the ball-and-stick plot of the 3-D anionic network of **1**, showing the 4-connected T-shaped building cluster $[WS_4Cu_3]^+$; (b) Packing diagram of **1** (ball-and-stick representation) viewed along the *c*-axis (gray sticks represent the CN^- bridges, and orange, red, and green balls represent the S, W, and Cu atoms, respectively); (c) The diamondoid topology of **1**.

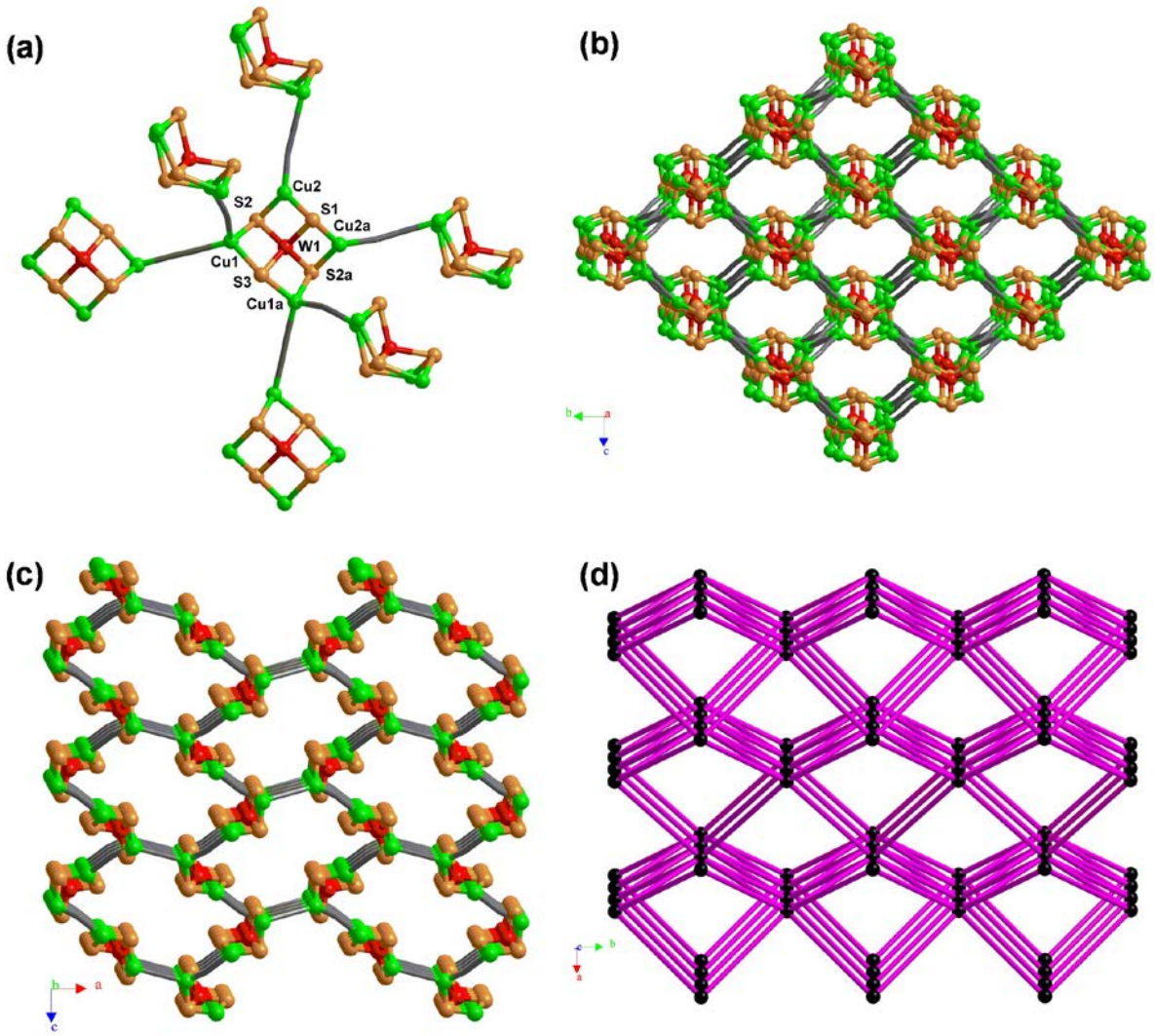

Figure 2. (a) Partial view of the ball-and-stick plot of the 3-D anionic network of **2**, showing the 6-connected planar 'open' cluster $[WS_4Cu_4]^{2+}$; (b) and (c) Packing diagrams of **2** (ball-and-stick representations) viewed along the *a*- and *b*-axes, respectively (gray sticks represent the CN^- bridges, and orange, red, and green balls represent the S, W, and Cu atoms, respectively); (d) The "ACS" topology of **2**.

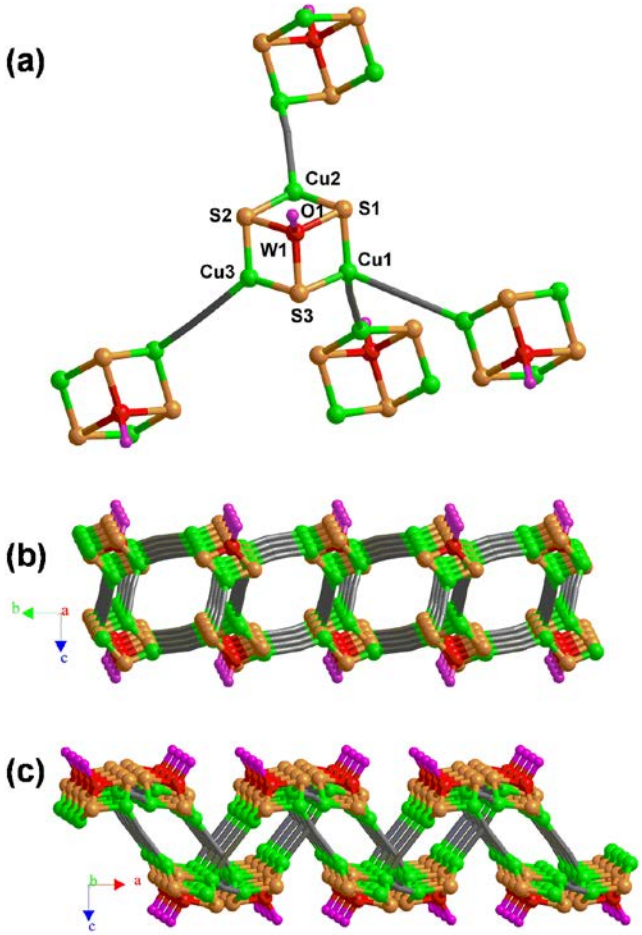

Figure 3. (a) Partial view of the ball-and-stick plot of the 2-D anionic network of **3**, showing the 4-connected nest-shaped cluster $[WOS_3Cu_3]^+$; (b) and (c) Packing diagrams of **3** (ball-and-stick representations) viewed along the *a*- and *b*-axes, respectively, showing the 2-D double-layer architecture (gray sticks represent the CN^- bridges, and orange, red, green, and pink balls represent the S, W, Cu, and O atoms, respectively).

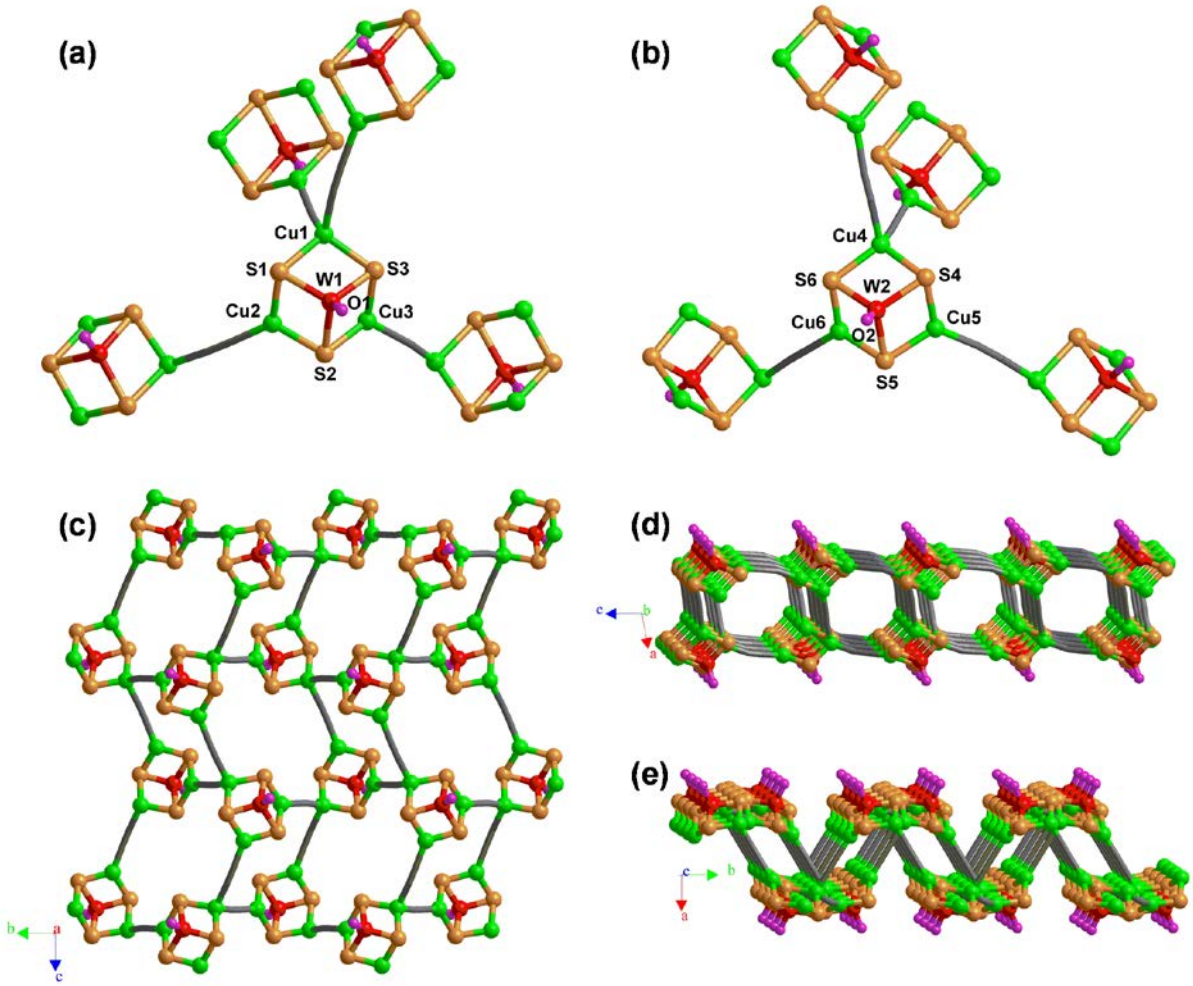

Figure 4. (a) and (b) Partial views of the ball-and-stick plots of the 2-D anionic network of **4**, showing the 4-connected nest-shaped clusters $[WOS_3Cu_3]^+$; (c) the 2D anionic network of **4** (ball-and-stick representation) viewed along the *a*-axis; (d) and (e) Packing diagrams of **4** (ball-and-stick representations) viewed along the *b*- and *c*-axes, respectively, showing the 2D double-layer architecture (gray sticks represent the CN^- bridges, and orange, red, green, and pink balls represent the S, W, Cu, and O atoms, respectively).

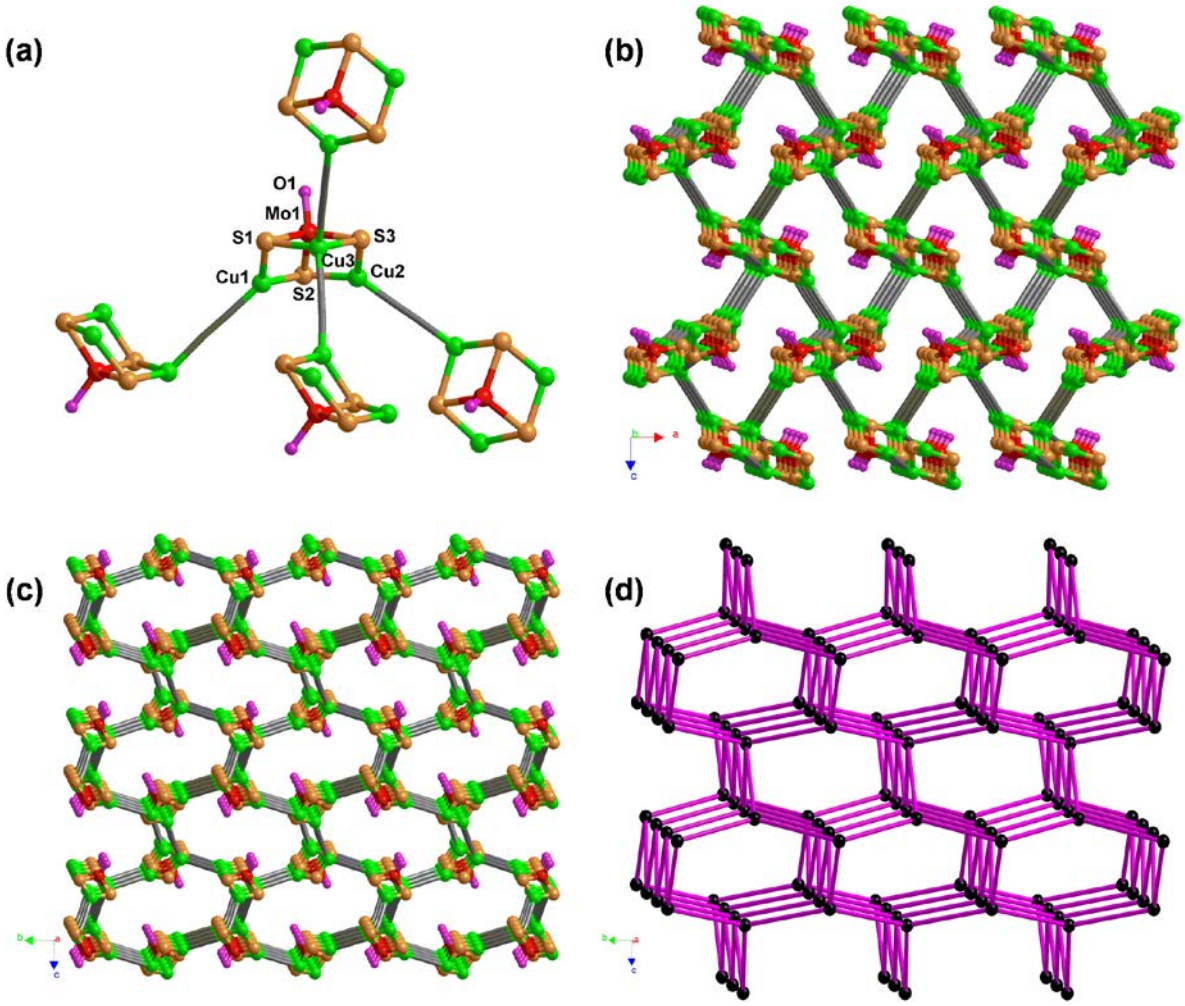

Figure 5. (a) Partial view of the ball-and-stick plot of the 3-D anionic network of **5**, showing the 4-connected nest-shaped cluster $[MoOS_3Cu_3]^+$; (b) and (c) Packing diagrams of **5** (ball-and-stick representations) viewed along the *b*- and *a*-axes, respectively (gray sticks represent the CN^- bridges, and orange, red, green, and pink balls represent the S, Mo, Cu, and O atoms, respectively); (d) The diamondoid topology of **5**.

Table 1. Crystallographic parameters and structure refinement data for **1**-**5**.

	1	**2**	**3**	**4**	**5**
Molecular formula	$C_{14}H_{28}Cu_3N_3S_4W$	$C_{15}H_{28}Cu_4N_4S_4W$	$C_{14}H_{28}Cu_3N_3OS_3W$	$C_{18}H_{36}Cu_3N_3OS_3W$	$C_{18}H_{36}Cu_3MoN_3OS_3$
Formula weight	741.16	830.73	725.09	781.20	693.30
Temperature (K)	150(2)	150(2)	150(2)	150(2)	150(2)
Wavelength (Å)	0.71073	0.71073	0.71073	0.71073	0.71073
Crystal system	orthorhombic	orthorhombic	orthorhombic	monoclinic	orthorhombic
Space group	$P2_12_12_1$	*P*nma	*P*bca	$P2_1/c$	$P2_12_12_1$
a (Å)	10.161(2)	20.342(4)	11.869(2)	29.179(6)	11.482(2)
b (Å)	11.539(2)	13.566(3)	15.672(3)	11.726(2)	15.535(3)
c (Å)	21.719(4)	9.877(2)	26.173(5)	16.300(3)	15.861(3)
α (°)	90	90	90	90	90
β (°)	90	90	90	100.21(3)	90
γ (°)	90	90	90	90	90
V (Å^3)	2546.5(8)	2725.7(10)	4868.5(16)	5488.8(18)	2829.2(9)
Z	4	4	8	8	4
ρ_{calc} (g cm^{-3})	1.933	2.024	1.979	1.891	1.628
μ (mm^{-1})	7.305	7.590	7.560	6.713	2.892
F (000)	1432	1599	2799	3055	1400
Reflections collected	12488	11956	18238	25233	10490
Unique reflections	5096	2589	4650	10097	5399
R_{int}	0.0345	0.0398	0.0452	0.0448	0.0452
No. parameters	206	120	226	523	263
GOF	0.983	1.071	1.174	1.132	1.080
R_1 [I > 2σ(I)]	0.0355	0.0585	0.0552	0.0596	0.0471
wR_2 [I > 2σ(I)]	0.0596	0.1491	0.1084	0.0862	0.1054
$\Delta\rho_{max}$ / $\Delta\rho_{min}$ (e Å^{-3})	0.885 / -1.036	2.605 / -1.304	1.030 / -0.919	0.940 / -1.211	0.531 / -0.881

For Table of Contents Use Only

Single Cyano-Ligand-Bridged Mo(W)/S/Cu Cluster-Based Frameworks: Reactant- and Stoichiometry-Dependent Syntheses and Nonlinear Optical Properties

Jinfang Zhang,[†] Yu Fang,[§] Yinlin Wang,[†] Weitao Chen,[†] Junyi Yang,[§] Yinglin Song,[§] Mark G. Humphrey,[‡] and Chi Zhang*[,†]

TOC graphic

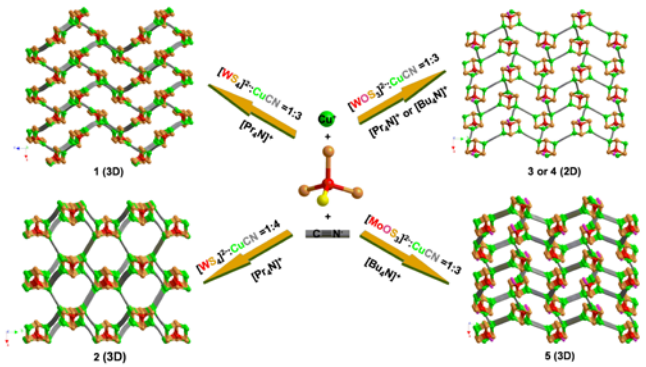

Five single cyano-bridged Mo(W)/S/Cu cluster-based frameworks were prepared for systematically examining the effects of varying the molar ratios of the starting materials and the types of cations, cluster building blocks and central metal atoms in cluster building blocks on the resultant architectures.
